High Strength Ceramic Substrates Based on Perlite and Foam Silicates for Filtration Membranes

N. P. Fadeeva[a, b], **M. V. Pavlov**[c], **I. A. Kharchenko**[a, f], **M. M. Simunin**[d, e],
K. A. Shabanova[f], **V. F. Pavlov**[c], and **I. I. Ryzhkov**[a, e], *

[a] *Institute of Computational Modeling, Siberian Branch, Russian Academy of Sciences, Krasnoyarsk, 660036 Russia*
[b] *Institute of Chemistry and Chemical Technology, Siberian Branch, Russian Academy of Sciences, Krasnoyarsk, 660036 Russia*
[c] *Specialized Design and Technological Bureau "Nauka" FRC KSC SB RAS,
50/45 Akademgorodok, Krasnoyarsk, 660036 Russia*
[d] *Federal Research Center, Krasnoyarsk Science Center, Siberian Branch, Russian Academy of Sciences,
Krasnoyarsk, 660036 Russia*
[e] *Siberian Federal University, Krasnoyarsk, 660041 Russia*
[f] *Kirensky Institute of Physics, Siberian Branch, Russian Academy of Sciences, Krasnoyarsk, 660036 Russia*
*e-mail: rii@icm.krasn.ru

Abstract—Samples of two-layer ceramics based on polydisperse powder of the pearlite mineral and foam silicates possessing high compressive strength up to 50 MPa, thermal stability up to 1150°C, and water permeability of 272 m^3/h m^2 bar have been obtained. According to the X-ray powder diffraction analysis, the supporting substrate material is X-ray amorphous. The average pore size of the supporting substrate is 40 μm, while the average pore size of the modifying layer is 17 μm according to the bubble method and electron microscopy. The obtained materials are promising for use as substrates of microfiltration, ultrafiltration, and nanofiltration membranes.

INTRODUCTION

Porous ceramic materials are widely used in membrane technologies for separating mixtures and obtaining pure substances, as well as in catalytic purification processes [1]. One of the most important applications of ceramic membranes is water treatment and wastewater treatment [2, 3]. Compared to polymeric materials, ceramic materials have greater mechanical strength, chemical and biological resistance, stability over a wide temperature range, and a longer service life [4]. In addition, they are often characterized by a narrower pore size distribution and higher porosity.

In baromembrane processes (microfiltration, ultrafiltration, and nanofiltration), multilayer ceramic membranes are used, in which the pore size and layer thickness decrease in passing from layer to layer [5, 6]. Coarse-porous ceramics are used as a base (substrate), on the surface of which macroporous and mesoporous coatings are formed in layers. For filtration applications, the main characteristics of the substrate are porosity, mechanical strength, and liquid permeability. The development of ceramic materials with an optimal combination of these properties is one of the urgent tasks of membrane science [7].

Previously, ceramic substrate membranes based on Moroccan perlite powder with organic additives and water were proposed [8, 9], which have high thermal stability up to 1000°C and porosity up to 40%. The application of a microfiltration layer by slip casting from a more dispersed perlite powder made it possible to achieve high adhesion to the substrate. It is shown that the obtained membranes ensured the retention of colloidal dyes used in the leather and textile industries, as well as particles in aqueous suspensions obtained during the cutting of silicon panels. In [10–12], highly porous permeable tubular ceramic materials with a macroporous surface layer were obtained. Crystalline silica powder was used as the starting material and an aluminosilicate binder was used. It has been shown that the resulting materials are characterized by high permeability and mechanical strength, hydrolytic and acid resistance, and can also be effectively used to remove ferric ions [13]. Modification of the resulting membranes by applying mesoporous selective layers using the sol-gel method was carried out [14]. The authors [15] developed a method for obtaining micro-

Table 1. Mass distribution of perlite powder particles in grams by size

Sizes of sieve cells, mm	Content, wt %
+0.315	5.0
−0.315 + 0.2	17.5
−0.2 + 0.16	19.9
−0.16 + 0.1	26.2
−0.1 + 0.071	10.7
−0.071 + 0.044	9.0
−0.044 + 0	11.7

filtration and ultrafiltration membranes using suspensions based on aqueous and alcoholic-aqueous solutions of carboxymethylcellulose deposited on an aluminosilicate substrate. The possibility of obtaining nanofiltration membranes by depositing nanopowders of titanium, aluminum, and magnesium oxides on ceramic substrates with macropores was demonstrated [16]. The technique for creating catalytic layers from cerium and zirconium oxides on the surface of tubular microfiltration membranes was developed [17]. The work [18] should also be mentioned, where asymmetric ceramic membranes with intermediate and active layers based on titanium oxide and boehmite nanofibers were obtained. The use of nanofibrous materials leads to a significant increase in permeability compared to traditional methods based on spherical nanoparticles. Symmetric ceramic membranes based on aluminum oxide nanofibers with a conductive carbon coating were proposed [19]. The possibility of changing the ion selectivity of membranes by varying the electric potential applied to the conducting surface was demonstrated [20, 21]. However, the use of such technologies in filtration processes requires the placement of a conductive selective layer on a strong macroporous substrate.

The aim of this work is to develop new types of high-strength ceramic materials based on perlite and foam silicates for use as substrates in the creation of microfiltration, ultrafiltration, and nanofiltration membranes. The choice of starting materials is due to their high thermal stability, mechanical strength, and chemical inertness to weak acids and weak alkalis. An important aspect is the commercial availability and prevalence of perlite, as well as the environmental friendliness of foam silicate, which is a material obtained as a result of processing technogenic raw materials [22, 23]. The obtained ceramic samples are characterized, and their mechanical strength and water permeability are studied.

EXPERIMENTAL

Perlite of the following chemical composition was used, wt %: SiO_2, 76.0; Al_2O_3, 11.7; Na_2O, 2.41; Cl, 0.64; K_2O, 6.38; CaO, 1.13; TiO_2, 0.19; Fe_2O_3, 1.33. Samples with a mass of 2 g, a diameter of 26 mm, and a height of 3 mm were formed from a polydisperse perlite powder with fractions of 0.315−0.044 mm, which passed through the sieves indicated in Table 1 at a pressing force of 10 kN on an IR-5047-50-03 installation (Tochpribor, Ivanovo, Russia). Water was used as a binder in an amount of 5 wt %. The granulometric distribution of powder particles was determined by the method of sieve analysis State Standard GOST 9758-86 [24].

The substrate samples were annealed in an electric furnace of the VTP 06 M1 00 type (ZAO IETs VNIIETO, Istra) at a temperature of 1100°C with a holding time of 20 min at a given temperature in the furnace atmosphere. The modifying foam silicate layer was applied by rolling the powder onto the substrate, followed by heat treatment at 900°C. The foam silicate powder consisted of regular spherical particles 10−20 μm in size.

X-ray powder difffraction analysis of the initial perlite powder and samples of porous ceramics obtained after heat treatment was carried out on a DRON-3 setup (Burevestnik Research Center, St. Petersburg) using CuK_α radiation in the 2Θ range 10°−70°. Thermoanalytical measurements were carried out on STA-449C equipment from NETZSCH (Germany) using differential scanning calorimetry (DSC) with simultaneous measurement of sample mass change and heat flux, as well as registration of mass spectra of evolved gases (CO_2, H_2O).

The surface structure, morphology, and linear dimensions of microrelief elements of cleavages of porous ceramic samples were evaluated using a Hitachi TM4000 Plus scanning electron microscope (Japan) in the backscattered electron mode at an accelerating voltage of 20 kV. The mechanical compressive strength was determined using an IR-5047-50-03 installation on cylindrical specimens 10 mm in diameter and 20 mm high by the pressure, at which they are destroyed. The chemical composition of perlite was determined by X-ray fluorescence analysis on a Bruker S2 RANGER spectrometer (Germany).

The open porosity of the material was measured by the increase in the mass of the sample upon impregnation with water. The pore size was determined by the bubble in water method (State Standard GOST R 50516-93) [25]. The maximum and average pore sizes were calculated using the formula:

$$D = 4\gamma \cos\theta / p,$$

where D is the pore size (m), γ is the surface tension of the liquid (for water, 72 mN/m), θ is the contact angle of wetting of the material (as a rule, for water it is assumed to be zero, since water wets silicate ceramics almost perfectly), p is the pressure (Pa). The measurement was carried out as follows: the sample was fixed in the holder, impregnated with water, and placed in a container with water to a depth of 7−10 cm. Then, air was supplied into the internal cavity of the sample and

its pressure was gradually increased. The pressure at which at least three pores open on the sample surface was fixed (the corresponding number of chains of gas bubbles is formed in the liquid layer). This pressure corresponds to the opening of pores of maximum size. A further increase of gas pressure in the sample volume leads to an intensive release of gas bubbles over the entire surface of the sample, which corresponds to the opening of medium-sized pores.

Membrane permeability was measured using a setup pumping distilled water through the membrane. The pressure was generated by a compressor, regulated using an AW20-F01C-A B pressure regulator (SMC, Japan), and controlled using an ISE40A precision pressure sensor (SMC, Japan). The volume of water that passed through the membrane was determined using a GX-800 balance (AND, Japan) (the mass was automatically recorded once per minute). The volume flow (velocity) of water (m³/s m²) was calculated using the formula

$$J = V/S,$$

where V is the volume of water passing through the membrane in one second (m³/s), S is the area of the membrane (m²). To approximate the experimental dependence of the volume flow J on the applied pressure difference ΔP (Pa), the Darcy law was used

$$\frac{\Delta P}{L} = \frac{\mu}{k} J \quad (1)$$

or its generalization to the case of nonlinear filtration (Forchheimer law) [26]

$$\frac{\Delta P}{L} = \frac{\mu}{k} J + \frac{\beta \rho}{\sqrt{k}} J^2. \quad (2)$$

Here, L is the membrane thickness, μ is the dynamic viscosity of water, k is the permeability coefficient, and β is the constant of the porous medium. Law (2) describes deviations from the Darcy law associated with the manifestation of inertial forces at high filtration rates. These deviations occur when the Reynolds number

$$Re = \frac{J \, D}{\mu/\rho}$$

exceeds some critical value [26].

In the range of applicability of Darcy's law, the permeability of membranes (m³/h m² bar) was calculated using the formula

$$K = \frac{k}{\mu L}. \quad (3)$$

Taking into account Eq. (3), Darcy's law (1) can be rewritten as $J = K\Delta P$. The following values of the parameters were used in the calculations below: $L = 3$ mm for perlite substrates and $L = 3.2$ mm for modified substrates, Pa s.

The physical properties of the resulting membranes (mechanical strength, porosity, pore size, and water permeability) were studied on the basis of a series of five substrate samples and five samples of two-layer membranes fabricated under the same conditions.

RESULTS AND DISCUSSION

It is known that the porosity of ceramic materials is significantly affected by the heat treatment temperature [1, 3]. Synchronous thermal analysis was carried out to determine the optimal sintering temperature for a macroporous perlite substrate. Several thermal effects are observed on the DSC curve (Fig. 1). In the range from 300 to 400°C, there is a weak exothermic effect due to the combustion of carbon from the surface of the sample with the release of carbon dioxide (curve m/z 44). The total mass loss in this temperature range, equal to 3.1%, consists of losses of carbon dioxide and sorption water (curve m/z 18). The release of carbon dioxide in a wide temperature range of 700–1150°C is probably due to carbon burnout from the inner surface of the sample, which, in turn, is associated with insufficient oxidizing capacity of the environment. This behavior is accompanied by an extension and a flat shape of the exothermic effect on the DSC curve. As follows from Fig. 1, the temperature range of 750–850°C corresponds to the transition of the sample to the pyroplastic state with a change in its heat capacity. It follows from the thermal analysis data that, in the temperature range of 1000–1150°C, no change in the mass of the sample is observed, while exothermic and endothermic effects are also absent. This served as the basis for choosing the annealing temperature of the samples in the indicated range (1100°C). It is known from the literature data [8, 9, 27–29] that, during sintering of pearlite substrates at temperatures above 1000°C, a sharp, almost complete, loss of sample porosity occurs. This may be, firstly, due to the use of various binders and additives, and, secondly, due to the finer fractional composition of the initial charge. In this work, the use of a higher annealing temperature is associated with the use of larger fractions of the initial pearlite powder in the range of 0.315–0.044 mm.

The choice of annealing temperature for the foam silicate layer is determined by the softening temperature of the foam silicate in the range of 750–910°C [30]. As a result of sintering at 900°C, the foam silicate softens, which contributes to its good adhesion to the substrate. At the same time, the spherical morphology of the particles is preserved, which allows the formation of a porous permeable layer (Figs. 3b and 3d).

According to X-ray powder diffraction data, the diffraction patterns of pearlite samples before and after annealing at 812 and 1100°C (Fig. 2, curves 1, 2, and 3, respectively) do not have clearly defined peaks. Thus, these samples are X-ray amorphous.
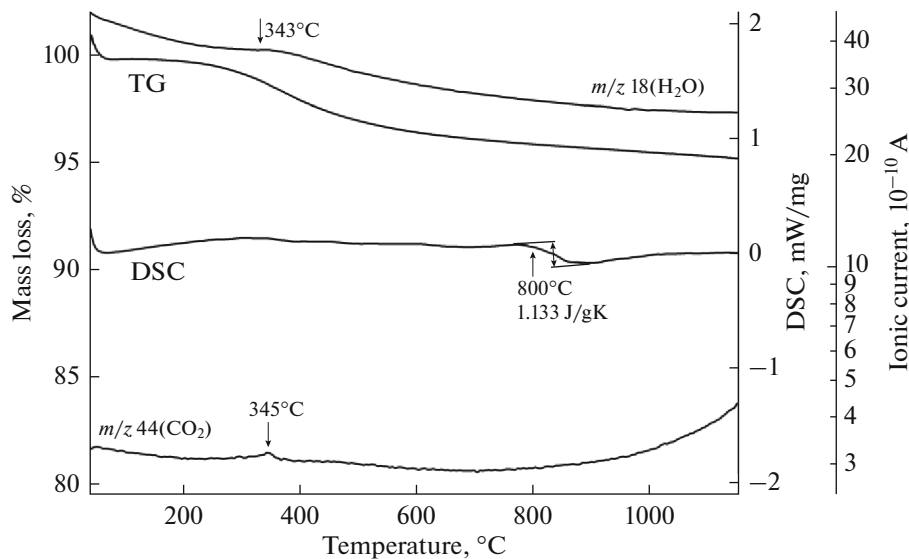
Fig. 1. TG and DSC curves for perlite samples combined with the mass spectrum of products released during heating (H_2O, CO_2).

Analysis of the SEM images of the membranes (Figs. 3a and 3c) shows that the gaps between the frame-forming particles of the substrate are located relatively uniformly over the sample surface. This indicates the uniform nature of the resulting porous structure. The maximum pore size is about 50 μm. In addition, it can be seen from the presented image that numerous contacts between the particles are observed after heat treatment. The sintering of particles in the liquid state due to surface tension forces without changing the volume content of the solid phase regions indicates compensation for shrinkage during sintering by foaming the sample due to the release of carbon dioxide. Sintering without changing the chemical composition of the particles, as follows from the

results of the work, contributes to an increase in the strength of porous ceramics.

After applying a modifying layer of foam silicate with a particle size of 10−20 μm to the carrier substrates, a uniform coating with a thickness of about 200 μm is achieved (Figs. 3b, 3d), which smooths the relief of the carrier substrate. During heat treatment, sintering of silicate foam particles occurs with the formation of a porous layer.

Data on the measurement of pore sizes by the bubble method are presented in Table 2. The diameter of large pores for silicate foam substrates is 50.1 ± 3.1 μm, and the diameter of medium pores is 39.6 ± 3.3 μm. After the substrates are modified with silicate foam, these values decrease noticeably and amount to 19.6 ± 0.6 μm for large pores and 16.8 ± 0.7 μm for medium pores, which agrees with electron microscopy data.

The compressive strength of the membranes is 50 ± 0.6 MPa for perlite substrates, while foam silicate samples of the same size have a tensile strength of up to 420 ± 5 MPa, depending on the pressing force. Since the strength of the product is usually limited by the compressive strength of the most brittle layer, it is assumed that the tensile strength of perlite substrates modified with a foam silicate layer has a similar compressive strength and is also 50 ± 0.6 MPa. Open porosity slightly decreases as a result of substrate modification and amounts to 30 ± 1 and $29 \pm 1\%$ before and after modification, respectively.

Figure 4 shows the dependences of the volume flow of water through the obtained ceramic membranes on the pressure difference in the range of 0.01−2 bar. At low pressures (up to 0.8 bar), the results for pearlite substrates are well described by the Darcy law (1) (curve *1*, permeability coefficient $k = 3.6 \times 10^{-12}$ m^2,
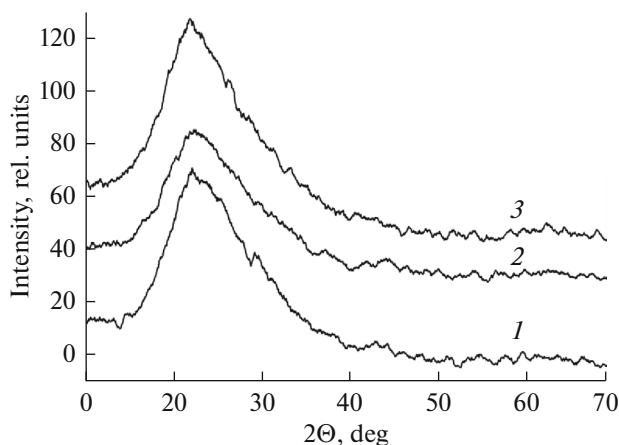

Fig. 2. X-ray powder diffraction patterns of pearlite samples before heat treatment (curve *1*) and after heat treatment at 812°C (curve *2*), 1100°C (curve *3*).
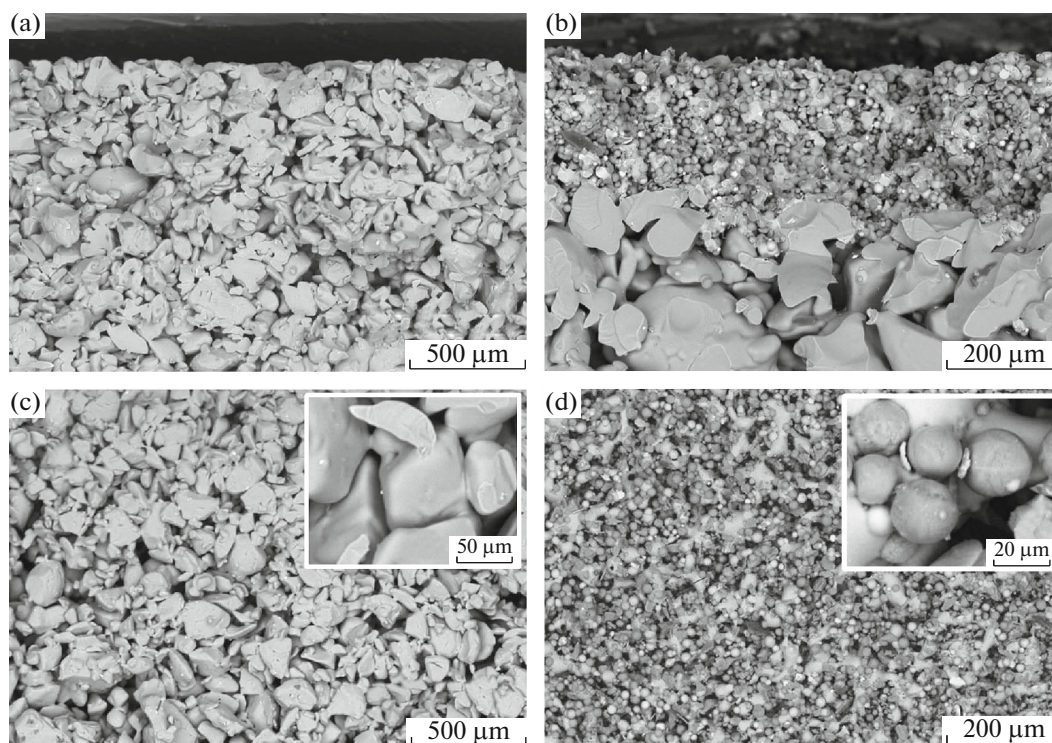
Fig. 3. SEM images of (a) cross section and (c) surface of the perlite substrate, and (b) cross section and (d) surface of the perlite substrate modified with a foam silicate layer.

water permeability $K = 485$ m^3/h m^2 bar). However, with increasing pressure, deviation from the linear law is observed. The dependence of the volumetric flow on the pressure difference in the entire considered pressure range is well described by the Forchheimer law (2) with parameters $k = 5.1 \times 10^{-12}$ m^2 and $\beta = 2$ (curve *2*). The value of the Reynolds number corresponding to the volume flow of water $J = 366$ m^3/h m^2

at a pressure difference $\Delta P = 0.8$ bar and the average pore size of the substrate $D = 39.6$ μm is Re = 4.03. This value is in the range of critical values of the Reynolds number Re = 3–10 that determine the upper limit of applicability of the Darcy law [26].

For substrates modified with a foam silicate layer, the dependence of the volume flow on the pressure difference is well described by the Darcy law (curve *3*,

Table 2. Physical and technical characteristics of ceramic substrates obtained here (1, 2) and in other studies (3–9)

| No.	Substrate material	D_{max}, μm	D_{av}, μm	Permeability, m^3/h m^2 bar	Compressive strength, MPa	Open porosity, %	Fraction size, μm	Heat resistance, °C
1	Perlite	50.1 ± 3.1	39.6 ± 3.3	485	50 ± 0.6	30 ± 1	44–315	1150
2	Perlite + silicate foam layer	19.6 ± 0.6	16.8 ± 0.7	272	50 ± 0.6	29 ± 1	44–315, 10–20	1150
3	Quartz sand [31]	20.6	25.3	89	5.05	26–28	200–400	850
4	Quartz sand + intermediate layer [31]	23.1	12.6	83	2.65	26–28	200–400, 40–70	850
5	Quartz sand + 30% dolomite [32]	–	18	53.6	16.2	45	0.3–60	1400
6	Perlite [27]	–	13	0.01	28.9	24.53	<180	1025
7	Perlite [8, 9]	–	6.64	1.797	1.2	41.8	200	1000
8	Perlite [28]	–	1.70	1.433	21.68	52.11	<45	950
9	Perlite + bentonite [29]	–	13×10^{-3}	0.03	21	52	–	–
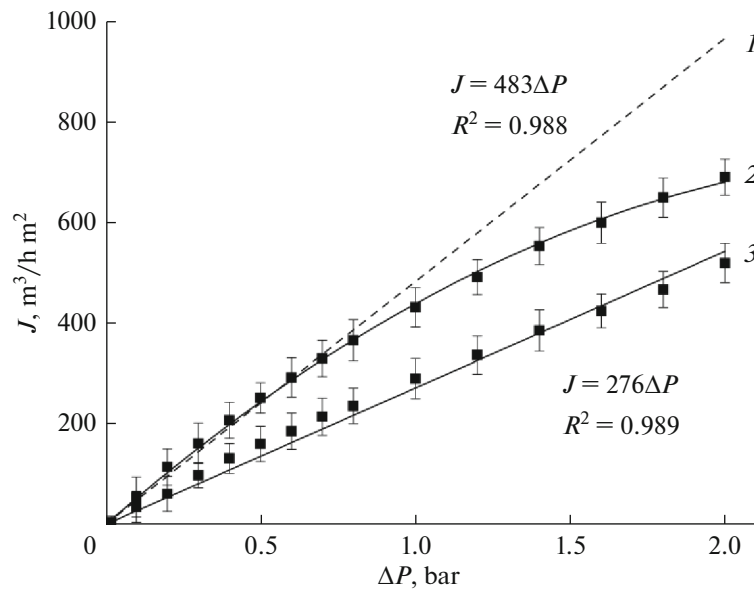
Fig. 4. Dependence of the volumetric water flow on the pressure difference for a perlite substrate (curves *1* and *2*) and a perlite substrate modified with a foam silicate layer (curve *3*).

permeability coefficient $k = 2.1 \times 10^{-12}$ m^2, water permeability $K = 272$ m^3/h m^2 bar). Thus, the modification of perlite substrates with a foam silicate layer leads to a decrease in liquid permeability (see Table 1). The Reynolds number corresponding to the volume flow of water at pressure difference $\Delta P = 2$ bar and the average pore size of the modified substrate $D = 16.8$ μm is Re = 2.6 and lies below the upper limit of applicability of Darcy law.

For comparison, Table 2 shows the characteristics of ceramic materials obtained in the works of other authors. In [31], quartz sand substrates with a modifying layer of SiO$_2$ particles were proposed. The fractional composition of the materials used is close to that used in this work. The resulting membranes have similar porosity and pore size of the modifying layer, but have lower values of strength, heat resistance, and liquid permeability in comparison to those obtained in this work. In the case of the formation of substrates from quartz sand and dolomite [32], a raw material with a more dispersed fractional composition was used. The authors managed to achieve a high porosity of 45% and heat resistance of 1400°C. However, the strength and fluid permeability values were not high relative to this work. In [27], substrate samples were made from perlite, which has a similar fractional composition (<180 μm) and a pore size of about 13 μm, but a significantly lower water permeability (0.01 m^3/h m^2 bar) compared to this work. The authors [7] obtained perlite-based samples with a high porosity of 41.8% and a pore size of 6.64 μm. They are characterized by relatively low strength and liquid permeability. Probably, these features are associated with the use of

organic additives, which increase the porosity, but greatly reduce the strength and permeability due to the formation of rather narrow pores as a result of heat treatment. In [28, 29], perlite substrates with a high porosity of 52%, sufficiently good mechanical strength, and low water permeability, which is due to the average pore size of 1.7 μm, were obtained. For the synthesis of membranes, a fraction of perlite powder with a particle size of less than 45 μm was used. Next, an ultrafiltration layer with a pore size of about 13 nm was applied from bentonite clay, followed by the use of the resulting membranes to purify aqueous solutions from dyes.

CONCLUSIONS

Methods for obtaining new types of high-strength and heat-resistant ceramic materials based on perlite and foam silicates have been proposed and developed. It has been established that the maximum values of strength and porosity correspond to substrates obtained from perlite with a granulometric composition in the range of 44–315 μm with an aqueous binder content of 5 wt % and molded at a pressing force of 10 kN. The porosity after heat treatment is 30%, and the compressive strength is 50 MPa. The modification of substrates with a foam silicate layer with a particle size of 10–20 μm in order to reduce the pore size and smooth the substrate relief does not lead to a decrease in the porosity and strength of the samples. It is shown that the application of a modifying layer causes a decrease in the water permeability of the substrates from 485 to 272 m^3/h m^2 bar, which is explained by a decrease in the size of through pores by almost a factor of two. The

dependence of the volume flow on the pressure difference in the range up to 2 bar for modified substrates is well described by Darcy's law, while for pearlite substrates deviations from this law are observed at pressures exceeding 0.8 bar.

Compared with similar materials presented in the literature, the developed ceramics are characterized by higher water permeability, compressive strength, and thermal stability. The obtained materials can be used as a basis for creating microfiltration, ultrafiltration, and nanofiltration membranes.

REFERENCES

1. K. Li, *Ceramic Membranes for Separation and Reaction* (John Wiley & Sons, Chichester, England, 2007).

2. A. V. Gorokhovskii, E. V. Tret'yachenko, V. G. Goffman, et al., Glass Ceram. **68**, 187 (2011). https://doi.org/10.1007/s10717-011-9349-

3. T. Arumugham, N. J. Kaleekkal, S. Gopal, et al., J. Environ. Manage. **293**, 112925 (2021).

4. V. Gitis and G. Rothenberg, *Ceramic Membranes: New Opportunities and Practical Applications* (Wiley-VCH. Weinheim, Germany, 2016).

5. M. C. Almandoz, C. L. Pagliero, N. A. Ochoa, et al., Ceram Int. **41**, 5621 (2015).

6. I. P. Garmash, Yu. N. Kryuchkov, and V. N. Pavlikov, Steklo Keram. **6**, 19 (1995).

7. X. Zhang, C. Bai, Y. Qiao, et al., Composites Part A **150**, 106629 (2021).

8. A. Majouli, S. Alami Younssi, S. Tahiri, et al., Desalination **277**, 61 (2011).

9. A. Majouli, S. Tahiri, Younssi S. Alami, et al., Ceram. Int. **38**, 4295 (2012).

10. A. I. Rat'ko, A. I. Ivanets, T. A. Azarova, et al., Zashch. Met. **44**, 217 (2008).

11. A. I. Rat'ko, A. I. Ivanets, E. A. Stepanova, et al., Prot. Met. Phys. Chem. Surf. **45**, 207 (2009). https://doi.org/10.1134/S2070205109020142

12. A. I. Ivanets and V. E. Agabekov, Pet. Chem. **57**, 117 (2017). https://doi.org/10.1134/S0965544117020037

13. A. I. Rat'ko, A. I. Ivanets, I. O. Sakhar, et al., Prot. Met. Phys. Chem. Surf. **48**, 553 (2012). https://doi.org/10.1134/S2070205112050085

14. A. I. Rat'ko, A. I. Ivanets, T. F. Kuznetsova, et al., Prot. Met. Phys. Chem. Surf. **46**, 227 (2010). https://doi.org/10.1134/S2070205110020103

15. T. P. Salikhov, V. V. Kan, E. M. Urazaeva, et al., Glass Ceram. **71**, 281 (2014). https://doi.org/10.1007/s10717-014-9669-z

16. Yu. M. Averina, A. Yu. Kurbatov, D. A. Sakharov, et al., Glass Ceram. **77**, 98 (2020). https://doi.org/10.1007/s10717-020-00248-x

17. N. N. Gavrilova, V. V. Nazarov, A. S. Sitnik, et al., Glass Ceram. **72**, 238 (2015). https://doi.org/10.1007/s10717-015-9764-9

18. X. B. Ke, H. Y. Zhu, X. P. Gao, et al., Adv. Mater. **19**, 785 (2007).

19. D. V. Lebedev, A. V. Shiverskiy, M. M. Simunin, et al., Pet. Chem. **57**, 306 (2017). https://doi.org/10.1134/S096554411704003X

20. D. V. Lebedev, V. S. Solodovnichenko, M. M. Simunin, et al., Pet. Chem. **58**, 474 (2018). https://doi.org/10.1134/S0965544118060075

21. I. I. Ryzhkov, M. A. Shchurkina, E. V. Mikhlina, et al., Electrochim. Acta **375**, 137970 (2021).

22. V. F. Pavlov and V. F. Shabanov, Ekol. Prom. Rossii **22**, 14 (2018).

23. O. N. Tsybulskaya, T. V. Ksenik, A. A. Yudakov, et al., Environ. Technol. Innovation **23**, 101567 (2021).

24. *GOST* (State Standard) *9758-86*: *Porous Inorganic Fillers for Construction Works. Test Methods* (Standartinform, Moscow, 2006).

25. *GOST* (State Standard) *R 50516-93. Polymeric Membranes. Method for Determining the Bubble Point of Flat Membranes* (Izdatel'stvo Standartov, Moscow, 1993).

26. K. S. Basniev, N. M. Dmitriev, and G. D. Rozenberg, *Underground Fluid Mechanics* (Moscow, 2005) [in Russian].

27. O. A. Al-Harbi, C. Özgur, and M. M. Khan, J. Ceram. Proc. Res. **17**, 275 (2016).

28. S. Saja, A. Bouazizi, B. Achiou, et al., J. Environ. Chem. Eng. **6**, 451 (2018).

29. S. Saja, A. Bouazizi, B. Achiou, et al., J. Eur. Ceram. Soc. **40**, 2453 (2020).

30. V. F. Pavlov, A. A. Shefer, and V. F. Shabanov, Glass Phys. Chem. **34**, 470 (2008). https://doi.org/10.1134/S1087659608040147

31. A. I. Ivanets, T. A. Azarova, V. E. Agabekov, et al., Ceram. Int. **42**, 16571 (2016).

32. C. Kadiri, A. Harabi, F. Bouzerara, et al., J. Aust. Ceram. Soc. **56**, 379 (2020).

Translated by V. Avdeeva